Computers and Electrical Engineering 83 (2020) 106591

Contents lists available at ScienceDirect

Computers and Electrical Engineering

journal homepage: www.elsevier.com/locate/compeleceng

An accurate cooperative positioning system for vehicular safety applications☆

João B. Pinto Neto[a], Lucas C. Gomes[a], Fernando M. Ortiz[a], Thales T. Almeida[a], Miguel Elias M. Campista[a], Luís Henrique M.K. Costa[a,*], Nathalie Mitton[b]

[a] GTA/PEE-COPPE/DEL-Poli, Federal University of Rio de Janeiro, Brazil
[b] National Institute for Research in Computer Science and Automatic Control, Lille, France

ARTICLE INFO

Article history:
Received 15 October 2018
Revised 6 December 2019
Accepted 13 February 2020

Keywords:
Cooperative GNSS positioning
Vehicular networks
DSRC
IEEE 802.11p

ABSTRACT

Typical Global Navigation Satellite System (GNSS) receivers offer precision in the order of meters. This error margin is excessive for vehicular safety applications, such as forward collision warning, autonomous intersection management, or hard braking sensing. In this work we develop a Cooperative GNSS Positioning System (CooPS) that uses Vehicle to Vehicle (V2V) and Vehicle to Infrastructure (V2I) communications to cooperatively determine absolute and relative position of the ego-vehicle with enough precision. To that end, we use differential GNSS through position vector differencing to acquire track and across-track axes projections, employing elliptical and spherical geometries. We evaluate CooPS performance by carrying out real experiments using off-the-shelf IEEE 802.11p equipment at the campus of the Federal University of Rio de Janeiro. We obtain an accuracy level under 1.0 and 1.5 m for track (where-in-lane) and across-track (which-lane) axes, respectively. These accuracy levels were achieved using a 2.5 m accuracy circular error probable (CEP) of 50% and a 5 Hz navigation update rate GNSS receiver.

1. Introduction

Vehicular communications support the development of various applications of Intelligent Transportation Systems (ITS), from infotainment to traffic safety. In this paper we focus on safe driving applications, most of which rely on information about location, speed, and direction of vehicles. That information is often obtained from Global Navigation Satellite System (GNSS) receivers. Vehicular safety applications, in addition to helping accident prevention, increase traffic law compliance, improve incident management, and facilitate crash investigations. Other than safe driving, applications which benefit from accurate vehicle positioning include autonomous vehicles, entertainment, traffic light control, assisted driving and detection of accidents [1–6]. Vehicle safety applications specifically require accurate positioning systems to improve vehicular navigation. This is the case of lane-level positioning and collision avoidance systems [7–10]. Nevertheless, the accuracy of GNSS receivers is often not enough. Moreover, it is compromised in urban canyons and under foliage by multipath, non-line-of-sight or complete blockage of GNSS signals [11].

☆ This paper is for regular issues of CAEE. Reviews processed and recommended for publication to the Editor-in-Chief by Associate Editor Dr. M. Shadaram.

* Corresponding author.
E-mail addresses: pinto@gta.ufrj.br (J.B. Pinto Neto), gomes@gta.ufrj.br (L.C. Gomes), fmolano@gta.ufrj.br (F.M. Ortiz), almeida@gta.ufrj.br (T.T. Almeida), miguel@gta.ufrj.br (M.E.M. Campista), luish@gta.ufrj.br (L.H.M.K. Costa), mitton@inria.fr (N. Mitton).

https://doi.org/10.1016/j.compeleceng.2020.106591
0045-7906/

Positioning systems based on GNSS are typically prone to errors in the order of meters, which exceed the acceptable maximum for various safe driving applications. For example, in a forward collision warning application, errors of this magnitude increase the risk of accidents, specially at higher speeds [12,13]. As another example, considering that streets and road lanes have widths between 2.5 and 3.5 m, a lane-level positioning system using only an autonomous single carrier (L1) GNSS receiver would be unreliable since errors and lane widths are in the same order of magnitude. Even though GNSS techniques such as DGNSS (Differential Global Navigation Satellite System), PPP (Precise Point Positioning), or RTK (Real Time Kinematics) respectively provide meter, centimeter, and millimeter accuracy, their performance is also affected by the number of visible satellites and by multipath propagation [14]. One way of circumventing these issues is to deploy a positioning system based on multiple inputs coming from collaborative sources, to compensate for individual errors. Those collaborative sources include Vehicle to Vehicle (V2V) and Vehicle to Infrastructure (V2I) communications, in-vehicle sensors, Light Detection and Ranging (LIDAR), cameras, and digital maps [15–18]. Typically, vehicular positioning solutions use subsets of those inputs. Thus, the number of devices to coordinate and the costs involved vary.

Positioning accuracy for vehicle safety is classified into three distinct levels: *which-road* (5.0 m), *which-lane* (1.5 m) and *where-in-lane* (under 1.0 m). The first means only to assess if the vehicles involved are on the same road. The second level of accuracy enables a vehicle to identify other vehicles that are traveling on the same or adjacent lanes, while the third level allows the identification of the vehicle's position inside the lane. Electronic Emergency Brake Light (EEBL), Forward Collision Warning (FCW), and Lane Change Advisor (LCA) are examples of vehicle safety applications that require the three accuracy levels, respectively [19].

In this paper we propose Cooperative GNSS Positioning System (CooPS), a system designed to provide *which-lane* accuracy. To obtain this accuracy level, CooPS uses (*i*) a combination of V2V and V2I communications over the Dedicated Short Range Communications (DSRC) band in a cooperative way, (*ii*) the well-known differential GNSS through the position vector differencing method, (*iii*) a novel technique to compute track and across track axes projections, and (*iv*) the assumption that GPS receivers located in the same road stretch share the same satellite constellation and ephemerids to overcome the low accuracy (of 10.0 m, typically) [20] of L1 GNSS receivers in Single Point Positioning (SPP) mode. One design requirement is to achieve accurate driving using only off-the-shelf GNSS receivers and, as a consequence, avoid compatibility issues imposed by additional sensors between vehicular equipment and the embedded GNSS. The use of fewer sensors reduces direct and indirect costs, like additional electrical wiring. Thus, another design goal is to use as few as possible data sources. We evaluate CooPS performance by carrying out experiments at the campus of Federal University of Rio de Janeiro (UFRJ) using IEEE 802.11p devices, installed along the roadway and inside the vehicle. The system is validated using the real distance between RSUs and Google Earth projections. The results show that CooPS achieves *where-in-lane* positioning accuracy with respect to cross-track axis and *which-lane* with respect to track axis using only a GNSS receiver as positioning input. As such, CooPS provides a low-cost solution, and in addition operates in any vehicle regardless of brand, cost or age.

This work is organized as follows. Section 2 positions CooPS with respect to related work. Section 3 introduces CooPS and provides an analysis of GNSS error sources. Section 4 details the CooPS proposal, the empirical methodology, and the geometric model considered. Field experiments are described in Section 5, as well as the results obtained in a real scenario, which serves as the proof of concept of CooPS. Finally, Section 6 provides closing remarks and discusses future work.

2. Related work

In this section, we focus on related works similar to the proposed system, i.e., designed to achieve *where-in-lane* level for navigation and collision warning applications, using multiple sensors or cooperative approaches.

Different positioning systems using multiple data sources have been investigated in the literature. The sources of information can be digital maps, GNSS, Inertial Measurement Units (IMU) and data acquired directly from the CAN bus of the vehicle [21]. Tsai et al. [22] propose IPC (Improving Positioning in real City environments), a cooperative system that combines an autonomous GPS and a camera to improve the accuracy of relative positioning in urban environments. IPC runs an algorithm that uses V2V communications in addition to the GPS and camera, to determine the position of the vehicle relative to its neighbors. In case of GPS failure, IPC relies only on the camera and V2V communications to perform navigation. Conversely, if the camera fails, GPS is used, performing mutual compensation between the navigation modes. IPC is a complete solution for relative positioning, nonetheless, it relies on the existence of a camera, V2V communications, and a GPS. CooPS on the other hand relies only on V2V and V2I communications, and a GPS to achieve accuracy below 1.5 m. Even considering that an additional camera does not add much complexity to the system, the reduction of 15% with respect to the raw GPS positioning error achieved by IPC yields an error greater than 4 m. This performance does not meet the requirements of vehicle safety applications.

Ansari et al. [23] propose a cooperative network architecture that is used to distribute differential corrections using the standard Radio Technical Commission for Maritime Services (RTCM) message format [24] and V2I communications. The Road Side Unit (RSU) receives geographic positions from an embedded GPS receiver, compatible with the RTK technique, and performs corrections using the data received from the nearest Continuous Operating Reference Station (CORS). The communications between the CORS and the RSU goes through the 3G cellular network that carries the correction messages using the Networked Transport of RTCM via Internet Protocol (NTRIP) [25]. This data is received at the OBUs also using the NTRIP protocol, which, in turn, allows the correction of the OBUs positions. The authors call this architecture Real-time Relative Positioning (RRP) and claim that it guarantees relative positioning of vehicles with centimeter precision, according

Table 1
Comparison between CooPS and related work.

Proposal	Error	Hardware	Network	Dead reckoning	Cost
CooPS	< 1.5 m	GNSS, OBUs and RSUs	V2V and V2I	No	Low
IPC [22]	> 4 m	GNSS, camera and OBUs	V2V	Yes	Medium
RRP [23]	Centimetric	RTK GPS, CORS station	3G	No	High
ASP [26]	< 15 m	GNSS and OBUs	3G	Yes	Low
VCCW [27]	N/A	GNSS, accelerometer and OBUs	V2V	Yes	Medium

to the experimental analysis carried out against various traffic scenarios. The proposal presents an accurate positioning system which meets the requirements of vehicle safety applications. Nevertheless, the system cost is high, due to the RTK GPS equipment and the need for a permanent communication with a CORS. In contrast, CooPS does not require permanent connection with a CORS and uses an off-the-shelf GNSS receiver.

Roth et al. [26] propose a collaborative positioning system also designed to reduce the number of sensors. They use an autonomous single carrier GPS installed in each vehicle as the only positioning sensor, and V2V communications to perform vehicle self-localization. The distance between each satellite and the Earth (pseudoranges) received by the vehicles in range are shared and, in case a vehicle's GPS receiver fails due to lack of satellite availability, neighboring vehicles act as sources of satellite data. The proposed Advanced Shared Pseudorange Algorithm (ASP) uses a least squares position estimation and the shared information to improve positioning accuracy, mitigating the problem of satellite unavailability in urban environments. ASP shares with CooPS low hardware cost and high degree of compatibility. Nevertheless, the accuracy achieved by ASP does not meet the requirement of vehicle safety applications, the position error ranging from 10 to 15 m.

Huang and Lin [27] propose a collision warning system based on three inputs: speed variation, direction change, and position interruption. The latter is defined as the time the system stays in the same position, which is equal to the GPS update period, for practical reasons. The proposed Vector Cooperative Collision Warning (VCCW) system evaluates the collision risk by considering a vehicle and all of its neighbors within the same coverage area, once per second. If there is a collision risk, a subsystem computes the safe braking distance and the time needed to reach this distance. The simulation of VCCW has shown safe braking distance errors below 3 cm. The work improves collision warning algorithms by also considering speed and direction variations, and position interruption over time. To accomplish that, VCCW takes account of the acceleration of the vehicle and the uses a vector-based algorithm to avoid collision even if vehicles change the course in a curve. Moreover, VCCW compensates for the time between two GPS acquisitions by adding the estimated distance traveled by the vehicle to its position. It also increases the accuracy with respect to errors introduced by the GNSS update rate. The performance of VCCW meets the requirements of vehicle safety applications: it is one of the few works that tackle the GNSS update rate issue. The main difference to the present work is that CooPS uses a novel geometric model, based on empirical results, to estimate the relative distance between vehicles. CooPS is simpler because it does not require coordinates transformations. Furthermore, compared with VCCW, which directly computes the distances between vehicles based on their GPS coordinates, CooPS provides a better accuracy by using an external reference (the RSU location). CooPS uses V2V and V2I communications, instead of only V2V, as VCCW does. We validate our proposal through real experiments. VCCW reports an error lower than 3 cm, but only for the determination of the safe braking distance, and only in simulations. The error was not measured in the experimental prototype; that is why it is shown as "not available" in Table 1.

Although most of the systems described above provide accuracy levels that meet *where-in-lane* requirements, their deployment is mainly relevant when GNSS fails to provide a reliable position. Thus, the main difference compared with CooPS is that it uses only the GNSS receiver as a positioning device, in the same conditions where other systems need additional sensors to achieve *where-in-lane* accuracy level. On the other hand, CooPS depends on a GNSS system and then, whenever it fails, e.g., when the vehicle enters a canyon, tunnel, or dense forest, the navigation may face interruptions. In this case, dead reckoning positioning techniques [28,29] can be used. Dead reckoning techniques do not require additional sensors and can operate using only data from available built-in sensors, such as wheel speed or steering angle sensors. Table 1 provides a brief comparison between CooPS and previous proposals of the literature.

3. Accurate positioning problem for safe driving applications

Fig. 1 shows the application scenario we consider in this paper. The key idea to produce accurate positioning is to combine information received from the GNSS with information received from other vehicles to accurately estimate the current position of the vehicle. To accomplish that, On-Board Units (OBUs), the mobile communication devices inside the vehicles, receive positioning information from fixed Road Side Units (RSUs), which we assume as surveyed base stations installed along a roadway. On the one hand, RSUs broadcast *precise* coordinates acquired at the time of their installation along the road, whereas OBUs acquire coordinates from their embedded GNSS receivers. To achieve high precision for the RSU geographic location (centimeter accuracy), the Differential Global Navigation Satellite System (DGNSS) technique is used to set the coordinates at the moment of RSU installation.

After receiving information from the RSUs using V2I communication, the application running in the OBU is able to find the ego-vehicle localization and, furthermore, compute the relative and absolute position in the current road stretch. To this

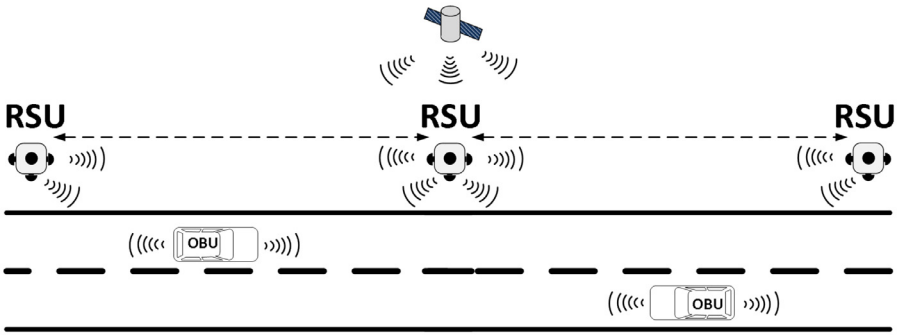

Fig. 1. Application scenario of CooPS where the Road Side Units, deployed along the road, broadcast their ground truth geographic position to the On-Board Units. This location information is used by the system embedded in the OBUs to determine the relative distance between vehicles.

end, CooPS must calculate, for every new position informed by the embedded GNSS receiver, the distances from its current position to the RSUs, which have absolute coordinates. Next, we describe the assumptions we make about the performance of GNSS receivers, so that the evaluation of the relative and absolute distance, the focus of CooPS, can be made.

3.1. GNSS error sources

GNSS is based on a constellation of satellites that send their orbital positions to receivers on Earth, providing geographic position and high precision time. Basically, GNSS receivers calculate positions estimating the distance between the satellite and the Earth (pseudoranges). The position accuracy varies depending on the visibility of available satellites as well as on signal reflections. More specifically, GNSS ranging errors can be caused by the variation of the speed of signal propagation (an effect of the ionosphere); pressure, temperature and humidity, which change the speed of light (troposphere effects); satellite orbit (ephemeris) data errors; satellite clock errors; intrinsic errors of the receivers; and multipath propagation [30]. Currently, four GNSS constellations are operational: the American GPS, Russian GLONASS, European GALILEO, and Chinese BeiDou. In this work, we use GPS equipment. Thus, hereinafter we use the term GPS instead of GNSS.

The geographic coordinates of any point around the globe can be determined by a single receiver (SPP mode) or by two GPS receivers working in differential mode (DGPS). The former, under ideal conditions, has an accuracy of around 10.0 m; whereas the latter, with the support of a reference ground station, can achieve centimeter accuracy [19]. A detailed analysis of the poor accuracy of GPS receivers working in SPP mode shows an assortment of error sources. Grewal et al. [30] analyze these error sources and point out that ephemeris and satellite clock errors slowly vary in time, but are more significant over long time intervals in the order of hours. They also conclude that, if two GPS receivers are close enough (less than some tens of km), the errors caused by the effect of the ionosphere and of the troposphere are highly correlated. Under this condition, the differential error of GPS receivers related to the ionosphere and the troposphere is very small (under 1 m). Considering the vehicular communication scenario, a driving safety application is typically concerned with events that occur in seconds or at most a few minutes. Moreover, the distances between RSUs should be less than 1 km, the theoretical radio communication range of IEEE 802.11p wireless devices [31], and around 300 m range for a better communication performance [32]. Hence, we assume that the relevant GPS error sources are multipath propagation and receiver noise, for the application scenario of vehicle safety applications.

3.2. Experiments using GPS receivers in SPP mode

Our first empirical experiments at the campus of UFRJ confirm that obtaining sub-metric positioning errors using GPS receivers operating in SPP mode is a challenge. We collect and analyze data from two GPS stationary stations separated by 160 m, shown in Fig. 2,[1] one located at the Technology Center 1 (CT1 Station) and another at the Technology Center 2 (CT2 Station). CT1 and CT2 Stations have single carrier (L1) autonomous GPS receivers with an accuracy of 2.5 m CEP in 50% of the measurements taken in a time interval of 24 h. Measurements were taken at both stations at one sample per second rate, during 24 h. Fig. 3a and b show the differences of acquired geographical coordinates (blue dots), in degrees from their mean (full red dot), denoted herein by *deviations*. The inner, intermediate and outer green circles represent boundaries corresponding respectively to the distances of 1, 5 and 10 m from the mean. We can observe that deviations greater than 10 m from the mean are more frequent at CT1 Station, which is in proximity of tall buildings (Fig. 2). This increases multipath reception errors and reduces the number of visible satellites.

The deviations shown in Fig. 3a and b confirm the hypothesis that GPS receivers working in SPP mode do not meet the requirements of vehicle safety applications. Nevertheless, such deviations occurred in a time interval of 24 h, which is

[1] Those are the stations of MagLev, the magnetic levitation train prototype developed at COPPE/UFRJ. CooPS will be used in the future to automate the train braking system.

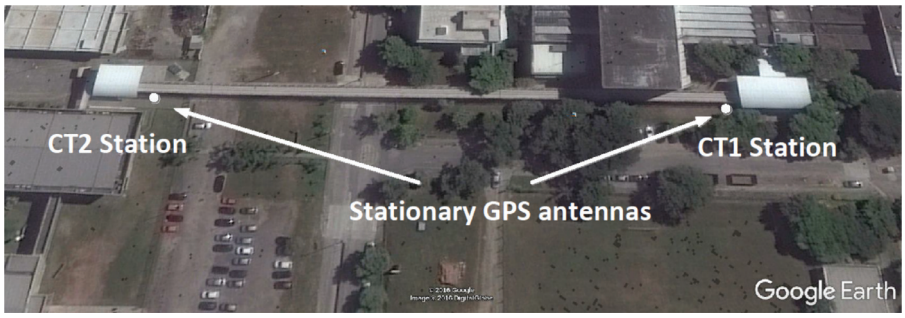

Fig. 2. Aerial view of the first experimentation site: CT1 and CT2 Stations.

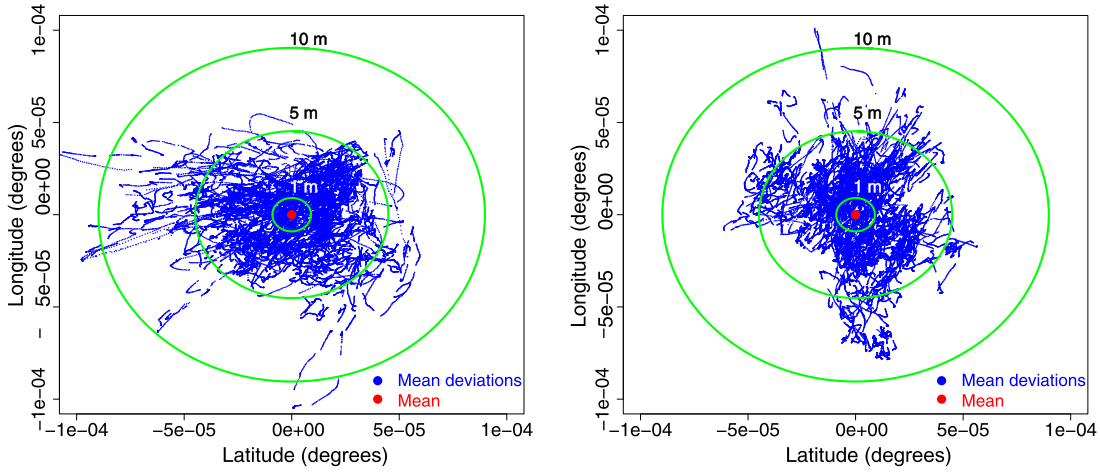

(a) CT1 Station. (b) CT2 Station.

Fig. 3. Mean deviations (errors) of coordinates acquired from GPS receiver stations during a 24-hour period. Green circles enclose deviations smaller than 1, 5, or 10 m, respectively.

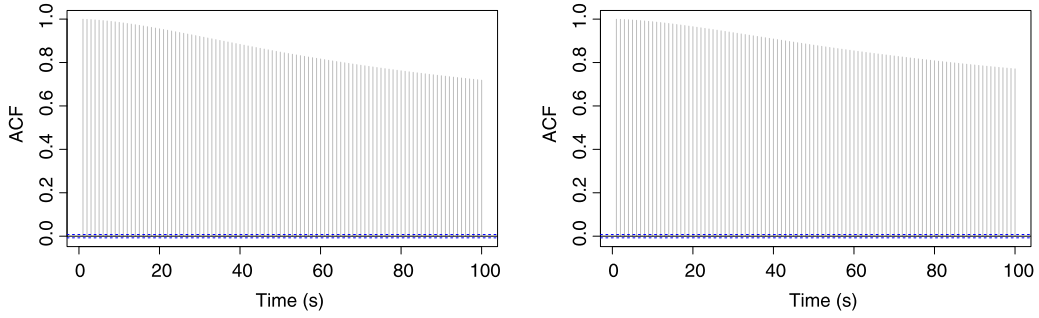

(a) CT1 Station. (b) CT2 Station.

Fig. 4. Time correlation of deviations acquired by the static GPS station receivers from a fixed coordinate at 90 s interval calculated using autocorrelation function (ACF) of time series of the errors.

prone to all error sources described in Section 3.1; and they are all computed as the distance to a fixed coordinate reference. Nevertheless, vehicle safety applications are related to events that occur at short time intervals, at short distances between the vehicles and within the same environment. Thus, we have set a maximum time interval between measures of 90 s (which corresponds approximately to a distance of 1400 m for a vehicle at 60 km/h) to evaluate time correlation of the deviations (errors). As the data was acquired at 1 s sample period, applying a proper operator we convert it to a time series and calculate the corresponding autocorrelation function (ACF) depicted in Fig. 4. As the figure shows, the deviations of both stations are highly correlated, which confirm the well-known behavior of static GPS receivers. As expected, a better time correlation for CT2 (Fig. 4b) station than CT1 station (Fig. 4a) can be observed due to different multipath conditions.

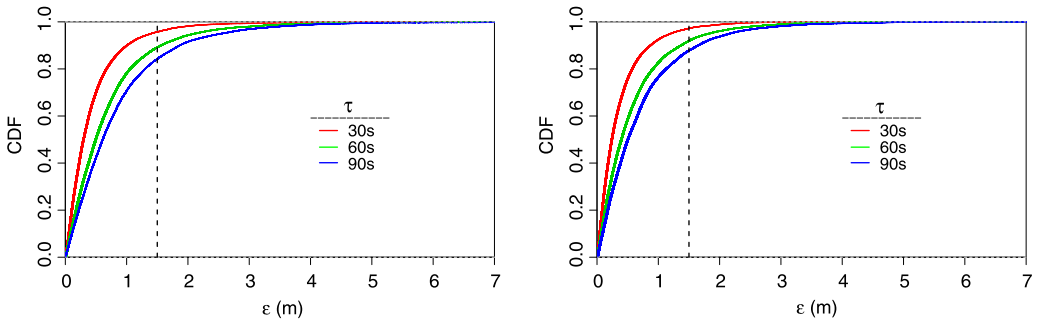

(a) CT1 station. (b) CT2 station.

Fig. 5. Cumulative density function (CDF) of ϵ to evaluate spatial correlation of multipath effect. The vertical dashed line at 1.5 m establish the maximum admitted value to meet vehicle safety applications requirements.

To evaluate the spatial correlation, we consider the difference between consecutive measurements instead of the absolute value between the samples and its 24-hour mean. This is equivalent to the use of the last measurement as reference coordinate, which reduces the deviation as consecutive measurements are expected to vary more smoothly. Let $p_0, p_1, \ldots, p_n$ be a sequence of coordinates acquired from a GPS receiver at a fixed rate and $d_0, d_1, \ldots, d_n$ the distances from these points to a fixed reference coordinate p_{ref}. Denoting τ a predefined time interval and ϵ_k as the error of the distances measured at time t_k and $t_{k+\tau}$, we have:

$$\epsilon_k = d_{k+\tau} - d_k. \tag{1}$$

Thus, considering $0 \leq \tau \leq 90$ s, ϵ_k is mainly produced by multipath carrier effect whose behavior we are interested to figure out if it meets the requirements of vehicle safety applications. For most applications, *which-lane* accuracy (1.5 m) is required. Analyzing the cumulative distribution function (CDF) of ϵ (Fig. 5) one can note that the 1.5 m threshold is achieved by more than 80% of the samples for CT1 station and almost 90% for CT2 station even for $\tau = 90$ s. Although these results are valid for static receivers, our proposition extends this concept to connected vehicles environment taking into account differential GPS through position vector differencing between a surveyed-coordinates RSU (static base) and an OBU (moving base), sharing the same satellite constellation and ephemerids. Our goal is to achieve *which-lane* positioning accuracy to meet the requirements of mostly vehicle safety applications within a dynamic window of 90 s.

4. The proposed cooperative GNSS positioning system

The main goal of CooPS (Cooperative GNSS Positioning System) is to provide at least *which-lane* accurate positioning, required by vehicle safety applications. CooPS adopts differential GPS through position vector differencing within the window of time in which vehicular security events occur. This simple difference of coordinates allows CooPS to operate with any GPS receiver device that just provides latitude, longitude, and speed information. The determination of the relative positions between vehicles and the absolute position of the vehicle itself within the stretch delimited by the RSUs is carried out using the projections of the vectors on the track and across-track axes, from now on denoted by road and lane axes. These projections are calculated using a new method based on elliptical and spherical geometry, shown ahead.

Fig. 6 illustrates the projection of the straight line between OBU_A and RSU_A over the road, R^A_Δ, and over the lane axis, L^A_Δ. Similarly, the projection of the vector between OBU_B and RSU_B produces the vectors R^B_Δ and L^B_Δ over the road and lane axis, respectively. Hence, considering that all vehicles use the same coordinate system, they only need to share its great circle projections (R_Δ to calculate the relative distance and L_Δ), therefore detecting a potential collision which would occur if the vehicles have the same L_Δ) value. CooPS geometric model uses the known surveyed positions of RSU_A and RSU_B to estimate the values of R_Δ and L_Δ. Therefore, besides calculating, for each new position received, the relative distance of the vehicles, CooPS also estimates their absolute position within the road segment. This feature is very useful for V2I safety applications.

As for the coordinate system, CooPS is based on the datum World Geodesic System 1984 (WGS84) reference ellipsoid to compute long distances for geographic coordinates (notation: $\phi = Latitude$, $\lambda = Longitude$). For some specific functions which operate over short distances, we use the spherical model in CooPS. In Fig. 6, points RSU_A and RSU_B represent two consecutive Road Side Units, located at geographic coordinates (ϕ_{RSU_A}, λ_{RSU_A}) and (ϕ_{RSU_B}, λ_{RSU_B}), respectively. OBU_A and OBU_B points represent the OBUs carried by two vehicles, currently located at the geographic coordinates ($\phi_{OBU_A}, \lambda_{OBU_A}$) and ($\phi_{OBU_B}, \lambda_{OBU_B}$), respectively. Note that the coordinates of the vehicles are informed by the GPS receivers of the OBUs. OBU_A and OBU_B travel at speeds v_a and v_b, respectively. The road axis, parallel to the great circle (GC) formed by RSU_A and RSU_B, is used to determine D_{RX}, the relative distance of vehicles regarding the traveling direction, whereas the lane axis is used to determine D_{LX}, the relative distance regarding to the lateral direction.

These relative distances can be calculated through the OBU's projections O_A, O_B, R_A, and R_B. Using V2I communications, the RSUs periodically send their ground-truth geographic coordinates to the OBUs. Rather than applying the simple differ-

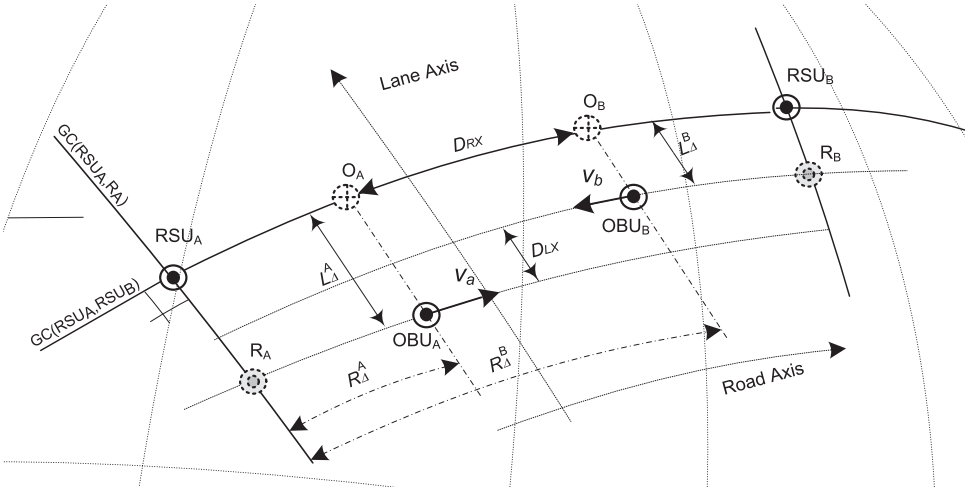

Fig. 6. Geometric model used by CooPS to determine the relative distances D_{RX} and D_{LX} between the OBUs with respect to road and lane axes, respectively. OBU_A and OBU_B represent vehicles traveling in different lanes at v_a and v_b speeds, respectively. OBU_A and OBU_B are in the same road stretch, delimited by the road-side units RSU_A and RSU_B. The arcs R^A_Δ, R^B_Δ, L^A_Δ, and L^B_Δ represent the road and lane axes displacement projections over their respective great circles (GCs).

ence to make positioning corrections, CooPS calculates the angular distance related to the projections of the acquired GPS positions over two orthogonal great circles (GCs), as represented in Fig. 6. These angular distances are used by CooPS to correct the OBU position in a simple and efficient way, avoiding the computational effort of coordinate transformations.

4.1. CooPS positioning algorithm

To obtain the distance between the two vehicles, CooPS first calculates the distances of the projections along the road axis defined by the GC that connects points RSU_A and RSU_B, denoted as GC(RSU_A, RSU_B). Then, it executes the same procedure regarding the lane axis, defined by the GC which is orthogonal to the first one, denoted by GC(RSU_A, R_A). Considering OBU_A, the system calculates, for each position informed by the GPS, the angular distances L_Δ and R_Δ from the points OBU_A and OBU_B to the GC(RSU_A, R_A). As Fig. 6 illustrates, these distances are the same as the $\overline{RSU_A O_A}$ and $\overline{RSU_B O_B}$ projections of the given points over GC(RSU_A, RSU_B). Therefore, the road axis relative distance D_{RX} between the OBUs is:

$$D_{RX} = |R^A_\Delta - R^B_\Delta|. \tag{2}$$

Similarly, with respect to the lane axis, we calculate the angular distances L^A_Δ and L^B_Δ from the OBU_A and OBU_B points to the circle GC(RSU_A, RSU_B). Hence, the lane axis relative distance D_{LX} between the OBUs is calculated as:

$$D_{LX} = |L^A_\Delta - L^B_\Delta|. \tag{3}$$

CooPS can also be used to determine the absolute position of the OBUs. The procedure is similar, except that there must be an external trigger, for example, a sensor on the vehicle, to establish a reference to correct the position with respect to both axes of the road.

CooPS assumes that there is a communication link between RSUs and OBUs along the road stretch and that the maximum distance between RSUs is smaller than the wireless network range. We only describe the procedure for determining the relative distance for OBU_A, since it is identical for OBU_B. Thus, three steps are performed before calculating L_Δ and R_Δ:

Step 1) *Compute the initial Azimuth between RSU_A and RSU_B.*
Using the elliptical model implemented by Vincenty solution [33] enhanced by Karney [34], the initial azimuth (bearing) β_{AB} from RSU_A at $(\phi_{RSU_A}, \lambda_{RSU_A})$ to RSU_B at $(\phi_{RSU_B}, \lambda_{RSU_B})$ can be computed as:

$$\beta_{AB} = \arctan 2(a, b), \tag{4}$$

where $a = \sin(\Delta_\lambda) \cdot \cos(\phi_{RSU_B})$, $b = \cos(\phi_{RSU_A}) \cdot \sin(\phi_{RSU_B}) - sin(\phi_{RSU_A}) \cdot \cos(\phi_{RSU_B}) \cdot \cos(\Delta_\lambda)$, and $\Delta_\lambda = \lambda_{RSU_B} - \lambda_{RSU_A}$.

Step 2) *Compute the initial Azimuth between RSU_A and OBU_A.*
Using Eq. 4, the initial azimuth β_{AA} is obtained from RSU_A at $(\phi_{RSU_A}, \lambda_{RSU_A})$ to OBU_A at $(\phi_{OBU_A}, \lambda_{OBU_A})$.

Step 3) *Compute the distance between RSU_A and OBU_A.*
The angular distance d_{AA} between points RSU_A at $(\phi_{RSU_A}, \lambda_{RSU_A})$ and OBU_A at $(\phi_{OBU_A}, \lambda_{OBU_A})$ can be obtained by using the Haversine formula, a spherical model, as:

$$d_{AA} = 2 \cdot atan2(\sqrt{c}/\sqrt{1-c}), \tag{5}$$

where $c = \sin^2(\Delta\phi/2) + cos(\phi_{RSU_A}) \cdot \cos(\phi_{OBU_A}) \cdot \sin^2(\Delta_\lambda/2)$, $\Delta\phi = \phi_{RSU_A} - \phi_{OBU_A}$, and $\Delta_\lambda = \lambda_{OBU_A} - \lambda_{RSU_A}$.

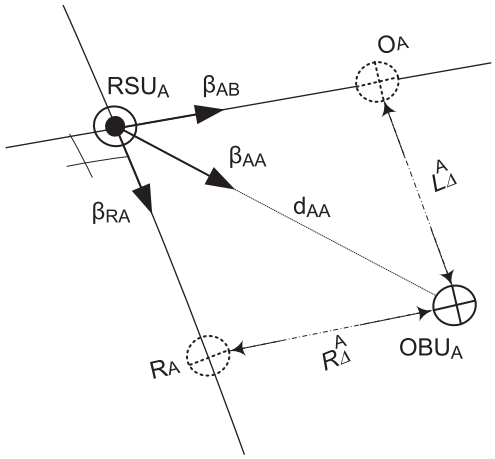

Fig. 7. Calculation of the projections R_Δ and L_Δ over the GC(RSU_A, RSU_B) and GC(RSU_A, R_A) using spherical trigonometric relations. R_Δ and L_Δ are function of distance and bearing between RSU_A and OBU_A and bearing of the corresponding GC projections.

We now have two GCs that intersect at point RSU_A, as required to determine the angular distances R^A_Δ and L^A_Δ, as shown in Fig. 7. Note that these projections over the respective GCs have a sign rule, given by the position of the point with respect to the GC. For example, if the point is on the right side of GC(RSU_A, R_A), like OBU_A, then R^A_Δ is negative. Otherwise, it is positive. The same occurs for GC(RSU_B, R_B).

Denoting the Azimuth $\beta_{RA} = \beta_{AB} + \pi/2$, the angular distance R^A_Δ from point OBU_A at $(\phi_{OBU_A}, \lambda_{OBU_A})$ to GC(RSU_A, R_A) can be calculated, given the initial azimuth β_{AA}, the angular distance d_{AA}, and the initial azimuth β_{RA}, using spherical trigonometry [35], as:

$$R^A_\Delta = \arcsin(d_{AA}) \cdot sin(\beta_{AA} - \beta_{RA})). \tag{6}$$

Similarly, the angular distance L^A_Δ from point OBU_A at $(\phi_{OBU_A}, \lambda_{OBU_A})$ to the GC(RSU_A, RSU_B) can be calculated, given the initial Azimuth β_{AA}, the angular distance d_{AA}, and the initial Azimuth β_{AB}, as:

$$L^A_\Delta = \arcsin(d_{AA}) \cdot sin(\beta_{AA} - \beta_{AB})). \tag{7}$$

R_Δ and L_Δ are calculated for every new position acquired from the GPS receiver and correspond to the distances to the respective GCs, the fixed references. These distances can be broadcast through Basic Safety Messages (BSMs) [36] to quickly estimate collision probability.

4.2. Considering the GPS update rate

Each GPS device has an update rate which defines the frequency new data is sent to the user application. Even for high precision devices, where the update period is 100 ms, when the vehicle drives at speeds above 120 km/h, the distance traveled during this refresh period is greater than 3 m. As this distance can compromise the accuracy of vehicle safety applications, we use a simple method derived from the CooPS geometry model to improve GPS accuracy.

Denoting t_0 as the time of the last GPS update, (ϕ_0, λ_0) the last coordinates, v_0 the last vehicle speed, the arc r traveled during the update interval T_{update} is:

$$r = (t - t_0) \cdot v_0, \;\; 0 \leq t - t_0 \leq T_{update} \tag{8}$$

where t is the current time. Denoting h_0 the last heading angle the latitude ϕ_c during this interval can be calculated as:

$$\phi_c = asin(sin(\phi_0) \cdot cos(r) + cos(\phi_0) \cdot sin(r) \cdot cos(h_0)). \tag{9}$$

Defining $a = sin(h_0) \cdot \sin(r) \cdot \cos(\phi_0)$ and
$b = cos(r) - sin(\phi_0) \cdot sin(\phi_c)$, the longitude λ_c during the T_{update} is:

$$\lambda_c = \lambda_0 + atan2(a, b). \tag{10}$$

Thus, the safety application does not need to wait the next update. Instead, it can call this algorithm to calculate the current coordinates (ϕ_c, λ_c), improving GPS accuracy.

5. Performance evaluation

We evaluate the performance of CooPS through real experiments conducted at a two-way street in the campus of UFRJ. Fig. 8 shows the experimental scenario. All GPS receivers are in line-of-sight conditions. Also, the GPS receivers share the

Fig. 8. Experimental scenario used for CooPS evaluation performance. Three separate road stretches were used, Lanes 1A, 1B, and 2. We used two fixed road-side units: RSU_A and RSU_B (figure produced using Google Earth).

Table 2
Equipment used in the experiments.

Hardware	Description
RSU	Cohda Wireless model MK5-RSU
OBU	Cohda Wireless model MK5-OBU
DSRC Antenna	2 × 5.9 GHz MobileMarkECO6-5500e
GNSS Antenna	1 × WELL-HOPE GPS/GLON-09B
Vehicle	2015 Peugeot 408

same environment and there are no tall buildings or trees within the experiment perimeter. The two RSUs are installed at a height of 1.5 m, separated by a ground distance of 407.64 m. The geographic coordinates of the RSUs ($\phi = Latitude$, $\lambda = Longitude$) were extracted from landmarks on the Google Earth map (a vertical white line for RSU_A and a light pole for RSU_B), their values are:

$$RSU_A : (\phi_{RSU_A} = -22.862084, \lambda_{RSU_A} = -43.22487),$$
$$RSU_B : (\phi_{RSU_B} = -22.860038, \lambda_{RSU_B} = -43.221572).$$

To evaluate the accuracy of CooPS regarding to the road axis, Lanes 1A and 1B were used whereas for the lane axis, Lanes 1A and 2 were used (Fig. 8). The distances from the RSUs to the center of Lanes 1A, 1B, and 2 are 2.68, 12.60, and 6.20 m, respectively. A vehicle with an embedded OBU traveled 15 times on Lane 1A, 15 times on Lane 2, and 30 times on Lane 1B at speeds between 20 and 60 km/h. The set of hardware used in the experiments is listed in Table 2. The CooPS elliptical geometry model was implemented using *GeographicLib* [37]. The RSUs and OBUs are equipped with single-carrier, 2.5 m accuracy CEP of 50% GPS receivers operating at 5 Hz navigation update rate. They are also equipped with two IEEE 802.11p radios used for V2V and V2I communications over the DSRC band, working at the power level of 23 dBm. Basic safety Messages between RSUs and OBU were sent on DSRC channel 178.

5.1. Results

In our experiments, we collect the values of R_Δ, L_Δ every time the vehicle travels the road stretch from RSU_A to RSU_B and from RSU_B to RSU_A. During that time, the vehicle speed and coordinates provided by the GPS receiver embedded in the OBU are also collected. To evaluate the precision of CooPS to estimate the relative distance to the road axis, we compute the values of R_Δ taking the vehicle traveling direction into account. When the vehicle goes from RSU_A to RSU_B (Lane 1A), R_Δ is computed from the RSU_A coordinates, until the vehicle overpasses RSU_B. This event is detected at the moment the vehicle crosses GC(RSU_B, R_B), as shown in Fig. 6. Similarly for Lane 1B, R_Δ is computed from the RSU_B coordinates until the vehicle overpasses RSU_A.

These values are compared with the distance between RSUs, calculated using absolute coordinates. Nevertheless, due to the GPS update rate combined with the vehicle speed, the signal changing detection of R_Δ happens after a random time interval, resulting in an additional distance, d_{cr}, given by:

$$d_{cr} = v_{cr} \cdot t_{cr}, \tag{11}$$

where v_{cr} is the vehicle speed when it crosses the GC and t_{cr} is a random fraction of the GPS update period. Assuming that t_{cr} is a random discrete variable with uniform distribution over [0, 200 ms] interval, where 200 ms is the update period of the used GPS, the expected value of d_{cr} is:

$$E(d_{cr}) = E(v_{cr}) \cdot E(t_{cr}). \tag{12}$$

Therefore, after extracting outliers and subtracting the corresponding expected values of d_{cr}, CooPS performance with respect to the road axis positioning error is shown in Fig. 9. Negative values mean an estimated distance shorter than the reference distance between the RSUs. The dotted red lines denote *which-lane* and green ones *where-in-lane* boundaries

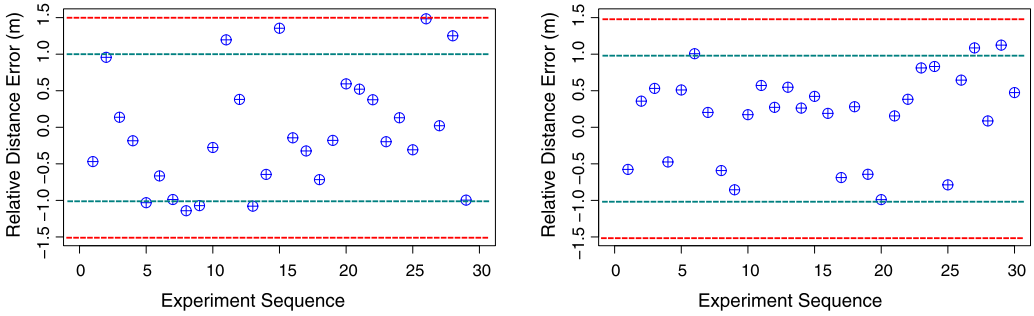

(a) Lane 1A Relative Distance Error. (b) Lane 1B Relative Distance Error.

Fig. 9. CooPS Road Axis Performance to estimate the distance between RSU_A and RSU_B. The dotted red lines denote *which-lane* and green ones *where-in-lane* boundaries.

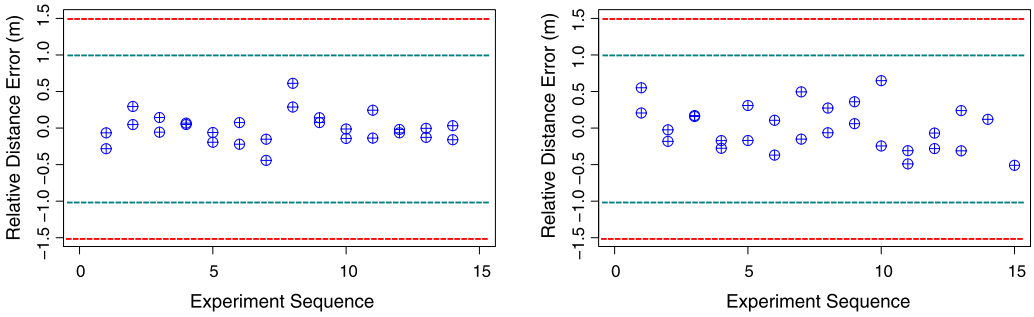

(a) Lane 1A. (b) Lane 2.

Fig. 10. CooPS lane axis error evaluation.

Table 3
Statistical data of road axis CooPS relative error acquired when the vehicle crosses the great circles.

Lane	Road axis relative error		
	Mean (m)	σ (m)	Conf. Int. (m)
1A	−0.06	0.78	[−0.36, 0.23]
1B	0.17	0.60	[−0.04, 0.40]

Table 4
Statistical data of lane axis CooPS relative error acquired when the vehicle crosses the great circles.

Lane	Lane axis relative error		
	Mean (m)	σ (m)	Conf. Int. (m)
1A	0.00	0.21	[−0.08, 0.07]
2	0.00	0.31	[−0.11, 0.12]

Note that the performance of CooPS with respect to the road axis meets *which-lane* requirements. A better performance is observed for Lane 1B (Fig. 9b which can be assigned by an average speed of experiment sequences lower than Lane 1A. This fact is confirmed by the numbers of Table 3, which shows smaller standard deviation (σ) and 95% confidence interval for the experiments over Lane 1B.

Assuming a negligible lateral displacement of the vehicle during the experiments, CooPS performance evaluation with respect to the lane axis was performed by calculating for each lane (1A and 2), the difference of the values of L_Δ at beginning (RSU_A) and at the end (RSU_B) of every experiment sequence, i.e. this difference must be zero, otherwise we have an error. Since lateral speed is zero, L_Δ has no additional distance at the end of sequence. Thus, after extracting outliers, the relative distance errors with respect to lane axis are shown in Fig. 10. We note a similar behavior of relative distance error for both experiment sequences, with a performance slightly better for Lane 1A, confirmed by the statistical data of Table 4. These values mean that CooPS exceeds *which-lane* requirements and provides *where-in-lane* accuracy level.

Fig. 11. CooPS absolute position validation. The landmarks 100, 200, 300 and 400 m are the corresponding ground positions from RSU_A. The errors are acquired from the comparison between CooPS estimation positions and Google Earth map positions (figure produced using Google Earth).

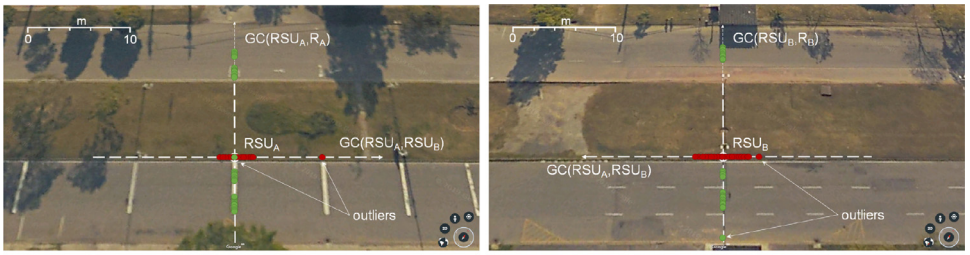

(a) Great Circle GC(RSU_A,R_A) crossing. (b) Great Circle GC(RSU_B,R_B) crossing.

Fig. 12. CooPS great circle crossing validation. The red points are the coordinates of R_Δ projections, green ones are the coordinates of L_Δ projections over GC(RSU_A, R_A) and GC(RSU_B, R_B) (white dashed lines). These points are acquired when the vehicle crosses the great circles GC(RSU_A, R_A) and GC(RSU_B, R_B) corresponding to Figs. a and b, respectively.

Table 5
Statistical data of position errors acquired by the comparison between CooPS absolute position estimation and Google Earth map ground position of the distances from RSU_A to the landmarks at 100, 200, 300 and 400 m.

Mark (m)	Position error		
	Mean (m)	σ (m)	Conf. Int. (m)
100	0.35	0.24	[0.22, 0.48]
200	0.32	0.28	[0.16, 0.47]
300	0.33	0.18	[0.23, 0.43]
400	0.34	0.22	[0.21, 0.46]

5.2. Validation

We validate the results plotting the R_Δ and L_Δ projections calculated by CooPS on Google Earth map in two scenarios. In the first one, we compare map ground position with CooPS estimated absolute position (R_Δ) from the RSU_A to points around 100, 200, 300 and 400 m along road stretch acquired when the vehicle traveled on Lane 1A (Fig. 11). We compare 60 points corresponding to 15 passages through 4 landmarks. The statistics shown in Table 5 reveal a similar behavior among landmarks position errors and confirm CooPS accuracy stability along the stretch limited by RSU_A and RSU_B.

In the second validation scenario, we compare CooPS position estimation with Google Earth map ground position when the vehicle crosses the great circles GC(RSU_A, R_A) and GC(RSU_B, R_B). We illustrate the results using the Google Earth map, as shown in Fig. 12. Fig. 12a and b are the zoomed area of the rectangle depicted in their upper left corners. The projections correspond to the nearest positions of the vehicle to the GCs in both Lane 1 (A&B) and Lane 2. The accuracy related to Road Axis (red dots) and related to the Lane Axis (green dots) can be evaluated comparing with the map scale. The figure also shows the outliers removed from the experiment's data.

6. Concluding remarks

This work presented CooPS, a cooperative positioning system that meets the accuracy requirements of vehicle safety applications. To achieve these requirements, CooPS employs IEEE 802.11p V2I and V2V communications, in a cooperation between vehicles and RSUs. CooPS uses differential GNSS through position vector differencing to compute the relative distance between vehicles and the surveyed-coordinates RSUs. The development of CooPS involved the analysis of GNSS receiver error sources and an experimental evaluation campaign where consecutive position errors over 24 h from two static GPS receivers were collected. CooPS has proved that the multipath error behavior of roving GPS receivers is similar to stationary ones in the vehicular environment if all the receivers share the same satellite constellation and ephemerids and considering

the short time during which vehicle interactions occur. CooPS also includes simple methods to handle the determination of relative and absolute position and to improve accuracy between updates. The system performance is confirmed by the field experiment results, using off-the-shelf IEEE 802.11p OBUs and RSUs. The results have shown a relative distance accuracy level under 1.5 m with respect to the road axis and under 1.0 m with respect to the lane axis. Despite the adoption of a single carrier GNSS as the unique positioning device, CooPS was able to provide positioning accuracy sufficient to deploy safety applications in vehicular environments, providing low cost and ease of installation, a step further with respect to state-of-art systems.

As future work we will develop a dead-reckoning subsystem to enable CooPS to use vehicle factory assembled sensors data to overcome GNSS unreliable data and unavailability due to urban canyons, dense forest canopies, and tunnels.

Declaration of Competing Interest

I declare that the authors do not have any conflicts of interest to report regarding this submission.

CRediT authorship contribution statement

João B. Pinto Neto: Conceptualization, Data curation, Formal analysis, Investigation, Methodology, Resources, Software, Supervision, Validation, Visualization, Writing - original draft, Writing - review & editing. **Lucas C. Gomes:** Data curation, Formal analysis, Software, Visualization, Writing - original draft, Writing - review & editing. **Fernando M. Ortiz:** Data curation, Formal analysis, Software, Visualization, Writing - original draft, Writing - review & editing. **Thales T. Almeida:** Data curation, Formal analysis, Software, Visualization, Writing - original draft, Writing - review & editing. **Miguel Elias M. Campista:** Conceptualization, Funding acquisition, Methodology, Supervision, Writing - original draft, Writing - review & editing. **Luís Henrique M.K. Costa:** Conceptualization, Funding acquisition, Methodology, Supervision, Writing - original draft, Writing - review & editing. **Nathalie Mitton:** Conceptualization, Funding acquisition, Methodology, Supervision, Writing - original draft, Writing - review & editing.

Acknowledgments

We are thankful to the Applied Superconductivity Laboratory Team for their support. This work was partially funded by FAPERJ grant number 202.932/2017, CNPq grant number 304142/2017-4, CAPES finance code 001, and grant numbers 15/24494-8 and 15/24490-2 of Fundação de Amparo à Pesquisa do Estado de São Paulo (FAPESP).

References

[1] Alam N, Dempster AG. Cooperative positioning for vehicular networks: facts and future. IEEE Trans Intell Transp Syst 2013;14(4):1708–17.
[2] Lu N, Cheng N, Zhang N, Shen X, Mark JW. Connected vehicles: solutions and challenges. IEEE Internet Things J 2014;1(4):289–99.
[3] Stenborg E, Hammarstrand L. Using a single band GNSS receiver to improve relative positioning in autonomous cars. In: IEEE intelligent vehicles symposium (IV); 2016. p. 921–6.
[4] del Peral-Rosado JA, López-Salcedo JA, Kim S, Seco-Granados G. Feasibility study of 5G-based localization for assisted driving. In: International conference on localization and GNSS (ICL-GNSS); 2016. p. 1–6.
[5] Abbas M, Karsiti M, Napiah M, Samir B, Al-Jemeli M. High accuracy traffic light controller for increasing the given green time utilization. Comput Electr Eng 2015;41:40–51.
[6] Aloul F, Zualkernan I, Abu-Salma R, Al-Ali H, Al-Merri M. iBump: smartphone application to detect car accidents. Comput Electr Eng 2015;43:66–75.
[7] Liu J, Cai B, Wang Y, Wang J. A lane level positioning-based cooperative vehicle conflict resolution algorithm for unsignalized intersection collisions. Comput Electr Eng 2013;39(5):1381–98.
[8] Bevly D, Cao X, Gordon M, Ozbilgin G, Kari D, Nelson B, et al. Lane change and merge maneuvers for connected and automated vehicles: a survey. IEEE Trans Intell Veh 2016;1(1):105–20.
[9] Sathiya P, Anandhakumar P. Probabilistic collision estimation for tracked vehicles based on corner point self-activation approach. Comput Electr Eng 2019;74:557–68.
[10] Riaz F, Jabbar S, Sajid M, Ahmad M, Naseer K, Ali N. A collision avoidance scheme for autonomous vehicles inspired by human social norms. Comput Electr Eng 2018;69:690–704.
[11] Zair S, Hégarat-Mascle SL, Seignez E. A-contrario modeling for robust localization using raw GNSS data. IEEE Trans Intell Transp Syst 2016;17(5):1354–67.
[12] Lambert A, Gruyer D, Pierre GS, Ndjeng AN. Collision probability assessment for speed control. In: 11th international IEEE conference on intelligent transportation systems; 2008. p. 1043–8.
[13] Neto JBP, Gomes LC, Castanho EM, Campista MEM, Costa LHMK, Ribeiro PCM. An error correction algorithm for forward collision warning applications. In: IEEE 19th international conference on intelligent transportation systems (ITSC); 2016. p. 1926–31.
[14] Zogg J.. GPS: Essentials of Satellite Navigation : Compendium : Theory and Principles of Satellite Navigation, Overview of GPS/GNSS Systems and Applications. U-blox AG; 2009. ISBN 9783033021396.
[15] Wisiol K, Wieser M, Lesjak R. GNSS-based vehicle state determination tailored to cooperative driving and collision avoidance. In: European navigation conference (ENC); 2016. p. 1–8.
[16] Jo K, Jo Y, Suhr JK, Jung HG, Sunwoo M. Precise localization of an autonomous car based on probabilistic noise models of road surface marker features using multiple cameras. IEEE Trans Intell Transp Syst 2015;16(6):3377–92.
[17] Hata AY, Wolf DF. Feature detection for vehicle localization in urban environments using a multilayer LIDAR. IEEE Trans Intell Transp Syst 2016;17(2):420–9.
[18] Scheel A, Knill C, Reuter S, Dietmayer K. Multi-sensor multi-object tracking of vehicles using high-resolution radars. In: IEEE intelligent vehicles symposium (IV); 2016. p. 558–65.
[19] Williams T, Alves P, Lachapelle G, Basnayake C. Evaluation of GPS-based methods of relative positioning for automotive safety applications. Transp Res Part C 2012;23:98–108.

[20] Shao M, Sui X. Study on differential GPS positioning methods. In: International conference on computer science and mechanical automation (CSMA); 2015. p. 223–5.
[21] Suhr JK, Jang J, Min D, Jung HG. Sensor fusion-based low-cost vehicle localization system for complex urban environments. IEEE Trans Intell Transp Syst 2017;18(5):1078–86.
[22] Tsai M-F, Wang P-C, Shieh C-K, Hwang W-S, Chilamkurti N, Rho S, et al. Improving positioning accuracy for VANET in real city environments. J Supercomput 2015;71(6):1975–95.
[23] Ansari K, Wang C, Wang L, Feng Y. Vehicle-to-vehicle real-time relative positioning using 5.9 GHz DSRC media. In: IEEE vehicular technology conference (VTC Fall); 2013. p. 1–7.
[24] Kalafus RM, Van Dierendonck A, Pealer NA. Special committee 104 recommendations for differential GPS service. Navigation 1986;33(1):26–41.
[25] He Z, Tang W, Yang X, Wang L, Liu J. Use of NTRIP for optimizing the decoding algorithm for real-time data streams. Sensors 2014;14(10):18878–85.
[26] Roth J, Schaich T, Trommer GF. Cooperative GNSS-based method for vehicle positioning. Gyroscopy Navig 2012;3(4):245–54.
[27] Huang CM, Lin SY. Cooperative vehicle collision warning system using the vector-based approach with dedicated short range communication data transmission. IET Intell Transp Syst 2014;8(2):124–34.
[28] Karlsson R, Gustafsson F. The future of automotive localization algorithms: available, reliable, and scalable localization: anywhere and anytime. IEEE Signal Process Mag 2017;34(2):60–9.
[29] Lassoued K, Bonnifait P, Fantoni I. Cooperative localization of vehicles sharing GNSS pseudoranges corrections with no base station using set inversion. In: IEEE intelligent vehicles symposium (IV); 2016. p. 496–501.
[30] Grewal MS, Andrews AP, Bartone CG. Global navigation satellite systems, inertial navigation, and integration. 3rd ed. New York, NY, USA: Wiley-Interscience; 2013.
[31] Demmel S, Lambert A, Gruyer D, Rakotonirainy A, Monacelli E. Empirical IEEE 802.11p performance evaluation on test tracks. In: IEEE intelligent vehicles symposium; 2012. p. 837–42.
[32] Teixeira FA, e Silva VF, Leoni JL, Macedo DF, Nogueira JM. Vehicular networks using the IEEE 802.11p standard. Veh Commun 2014;1(2):91–6.
[33] Vincenty T. Direct and inverse solutions of geodesics on the ellipsoid with applications of nested equations. Surv Rev 1975;23(176):88–93.
[34] Karney CFF. Algorithms for geodesics. J Geodesy 2013;87(1):43–55.
[35] Veness C. Movable Type Scripts; 2016 (accessed November, 2019). http://williams.best.vwh.net/avform.htm.
[36] Liu W, Li B. Research on the mechanism of intelligent transportation systems on improving road safety. Berlin, Heidelberg: Springer Berlin Heidelberg; 2015. p. 257–63. ISBN 978-3-662-46466-3.
[37] Karney C.. Geographiclib; 2015 (accessed November, 2019). https://geographiclib.sourceforge.io/.

João B. Pinto Neto (*in memoriam*) received his Electronic Engineering degree from Universidade Federal do Rio de Janeiro (UFRJ), Brazil, in 1979; his M.Sc. degree on Information Technology from Universidade Federal do Amazonas (UFAM), Brazil, in 2011. He was a full time professor with the Instituto Federal de Educação, Ciência e Tecnologia of Rondônia (IFRO), and a graduate student with UFRJ until he sadly passed away on April 2019.

Lucas C. Gomes received his B.Sc. degree in Computer and Information Engineering from Federal University of Rio de Janeiro (UFRJ), Brazil, in 2018. He is currently a M.Sc student at the Electrical Engineering Program of COPPE/UFRJ. His major research interests are Vehicular Networks, Intelligent Transportation Systems, Machine Learning and Internet of Things.

Fernando M. Ortiz received his M.Sc. degree in Electrical Engineering from Federal University of Rio de Janeiro (UFRJ), Brazil, in 2016, and his bachelor degree from Universidad Católica de Colombia (UCC), Bogotá, in 2011. He is currently working toward Ph.D. degree at COPPE/UFRJ, in Brazil. His major research interests are on sensor networks, Internet of Things and vehicular networks.

Thales T. Almeida received his M.Sc. degree in Computer Science from Federal University of Viçosa (UFV), Brazil in 2016, and his B.Sc. degree in Information Systems from Doctum College, in 2013. He is currently a Ph.D. candidate at COPPE/UFRJ, in Brazil. His major research interests are on vehicular networks, Intelligent Transportation Systems and Internet of Things.

Miguel Elias M. Campista received his D.Sc. degree in Electrical Engineering from UFRJ in 2008 and spent 2012 with the LIP6 lab at Sorbonne Université, Paris, France, as invited professor. He is an associate professor at the Universidade Federal do Rio de Janeiro (UFRJ), Rio de Janeiro, Brazil, since 2010. His major research interests include network science and wireless networking.

Luís Henrique M. K. Costa received his Eng. (Cum Laude) and M.Sc. degrees in electrical engineering from Universidade Federal do Rio de Janeiro (UFRJ), Brazil, and the Dr. degree from Université Pierre et Marie Curie (Paris 6), Paris, France, in 2001. Since August 2004, he has been an associate professor with COPPE/UFRJ. He has served in the TPC of many IEEE conferences for several years and is an associate editor of IEEE Communications Surveys and Tutorials since 2007. His major research interests are in the areas of Internet routing and vehicular networks.

Nathalie Mitton received the M.Sc. and Ph.D. degrees in Computer Science from INSA Lyon in 2003 and 2006 respectively. She received her Habilitation à diriger des recherches (HDR) in 2011 from Université Lille 1. She is currently an Inria full researcher since 2006 and from 2012, she is the scientific head of the Inria FUN team. Her research interests focus on self-organization from PHY to routing for wireless constrained networks. She has published her research in more than 40 international revues and more than 100 international conferences. She is involved in the set up of the FIT IoT LAB platform, the H2020 VESSEDIA or CyberSANE projects and in several program and organization committees such as Infocom 2020&2019, PerCom 2020&2019, DCOSS 2019. Orcid : 0000-0002-8817-6275.